DOI: https://doi.org/10.15625/0868-3166/22706

# Observability of frequency shift induced by multielectron polarization in the high-order harmonic generation emitted from CO molecules

Kim-Ngan H. Nguyen<sup>1,2</sup>, Doan-An Trieu<sup>1</sup>, Cam-Tu Le<sup>3</sup>, Hien T. Nguyen<sup>4</sup>, and Ngoc-Loan Phan<sup>5,†</sup>

E-mail: †loanptn@hcmue.edu.vn

Received 15 April 2025; Accepted for publication 16 May 2025; Published 29 May 2025

**Abstract.** Studying the effects caused by core electrons of highly polarizable atoms and molecules is essential since interactions between external fields and matter primarily occur in the outer electron shell, but the contribution of the core electrons has been revealed in recent studies. Therefore, investigating the multielectron polarization (MEP) in the high-order harmonic generation (HHG) emitted from matter when interacting with intense, ultrashort laser pulses has attracted significant attention. In our latest work, we have shown that when interacting with a few-cycle laser pulse, MEP induces significant shifts in the HHG peaks of the CO molecules. However, the parameter ranges of the laser pulse, allowing the observation of these peak shifts, have not yet been thoroughly examined. In this paper, by simulating the HHG emitted from the CO molecule under interactions with few-cycle laser pulses of different parameters, we demonstrate that the laser pulse duration should be greater than three cycles and less than six cycles. Furthermore, the carrier-envelope phase of the laser pulse should be within the ranges of  $(2\pi/3, 7\pi/6)$  and  $(5\pi/3, 2\pi)$ . These optimal regions guide experiments in choosing laser settings to observe core-electron effects on the HHG spectrum via peak shifts.

Keywords: high-order harmonic generation; multielectron polarization; core electrons; CO molecule; harmonic peaks' shift; frequency shift.

Classification numbers: 31.15.xv; 42.65.Ky; 42.65.Re.

<sup>&</sup>lt;sup>1</sup>Duy Tan University, Ho Chi Minh City, Vietnam

<sup>&</sup>lt;sup>2</sup>Nuclear Training Center, Vietnam National Atomic Energy Commission, Hanoi, Vietnam

<sup>&</sup>lt;sup>3</sup>Ton Duc Thang University, Ho Chi Minh City, Vietnam

<sup>&</sup>lt;sup>4</sup>Tay Nguyen University, Buon Ma Thuot City, Vietnam

<sup>&</sup>lt;sup>5</sup>Ho Chi Minh City University of Education, Ho Chi Minh City, Vietnam

#### 1. Introduction

The study of the structure and dynamics of matter has garnered significant interest in the fields of physics and chemistry. Advances in high-intensity, ultrashort laser pulse generation techniques have allowed researchers to delve deeper into the properties of matter, particularly in exploring ultrafast movements at the atomic and molecular scales [1–3]. When intense ultrashort laser pulses interact with matter, one of the prominent nonlinear optical phenomena that emerges is high-order harmonic generation (HHG) [4,5]. HHG is the emission of photons whose frequencies are multiples of the driving laser frequency, and the multiples are called the harmonic order. With the recent availability of strong-field long-wavelength laser sources, HHG photons can now reach the extreme ultraviolet (XUV) and even the soft X-ray spectral regions [6,7]. Moreover, HHG is a unique source of attosecond (10<sup>-18</sup> s) laser pulses, which are valuable tools for probing ultra-fast electron dynamics in atoms and molecules [8–14].

The HHG spectra exhibit a typical structure [4,5]. In the perturbative region, which corresponds to low harmonic orders, the intensity of HHG decreases rapidly. As the harmonic order increases, the intensity remains nearly constant, forming a plateau region that provides insight into atomic and molecular structures and dynamics [8–14]. The plateau ends at the cutoff, beyond which the HHG intensity drops sharply.

The mechanism of HHG can be intuitively understood within the framework of the classical three-step model, which comprises the following steps: (i) initially, a strong laser electric field induces tunnel ionization of atoms or molecules, freezing electrons; (ii) the liberated electron then propagates in the laser field, gaining kinetic energy, and when the laser field reverses direction, the electron is driven backward; and (iii) recombines with the parent ion, releasing its accumulated energy in the form of high-order harmonic photons [4, 5, 15]. According to this mechanism, the HHG spectrum is predominantly contributed by electrons from the outermost shell of the atom or molecule, while core electrons are typically considered "frozen" and do not participate in the HHG [4, 5]. This assumption is reasonable since, in the tunnel ionization mechanism, the ionization probability depends exponentially on the binding energy of the electron; thus, the probability of ionization from the outermost shell is exponentially higher than that from deeper shells [16].

However, some recent experimental measurements cannot be explained solely by the outermost atomic or molecular shells; they also require taking into account the contributions of core electrons [10, 11, 17–19]. A notable effect of core electrons is multielectron polarization (MEP), where the core electrons can be polarized in response to a laser electric field [20]. It has been demonstrated that MEP significantly affects various high-order nonlinear optical processes [18, 21–25], including HHG [14, 26–33]. Numerous studies have shown that MEP alters the HHG intensity near the cutoff region [28, 30, 31], modifies the intensity in the minimum [27] or induces a Cooper minimum [26], shifts the position of the minimum [29], and affects even-to-odd ratio, i.e. the intensity ratio between even and adjacent odd harmonic orders [32, 33]. More recently, it has been demonstrated that MEP has a significant influence on the peak structures in the HHG spectra emitted from solid crystals [14].

A prominent feature of the HHG spectrum is the harmonic peaks' position. When an atom or symmetric molecule interacts with a linearly polarized multi-cycle laser pulse, the HHG spectrum typically displays sharp peaks at odd harmonic orders [34]. This characteristic stems from the spatiotemporal symmetry of the laser–target (atom or molecule) system under the symmetry

transformation  $P: \mathbf{r} \to -\mathbf{r}, t \to t + T_0/2$ , where  $\mathbf{r}$  is the electron position and  $T_0$  is a laser period. Any breaking of this symmetry results in the emergence of even-order harmonics [34]. Symmetry-breaking factors may originate from an asymmetric electric field, such as the addition of a static field or a second laser with a different frequency, or from the intrinsic asymmetry of a polar molecule itself [34–39]. If the magnitude of the symmetry-breaking factor varies, the intensities of both even and odd harmonics also change accordingly [32, 38–41]. Recently, in Ref. [32], we have demonstrated that MEP significantly alters the even-to-odd ratio, defined as the ratio of the intensity of an even order to that of its adjacent odd order. The calculated even-to-odd ratio agrees well with experimental measurements only when MEP is taken into account.

Recent advancements in laser technology have successfully generated ultrashort laser pulses with durations spanning only a few optical cycles. In such scenarios, the HHG peaks may no longer align with integer harmonic orders [42–44]. In our recent work [45], we have demonstrated that MEP induces a frequency shift of the HHG peaks emitted from the CO molecule when interacting with few-cycle laser pulses. Specifically, MEP causes a frequency shift of up to 1.24 eV for harmonics near the cutoff region. Furthermore, we found that the frequency shift of HHG peaks induced by MEP under few-cycle laser fields, and the change in the even-to-odd ratio caused by MEP under multicycle laser fields, originate from the same underlying mechanism—namely, the MEP-induced phase distortion of adjacent attosecond bursts observed in the time domain. Thanks to this common origin, in Ref. [45], we indirectly confirmed the MEP-induced frequency shift of harmonic peaks by leveraging the odd-even HHG emitted from oriented CO molecules interacting with multi-cycle laser pulses [19, 46]. However, we still recommend that HHG experiments involving oriented polar molecules exposed to few-cycle pulses should be conducted to provide a more direct confirmation.

It is worth noting that, to observe the MEP-induced shift of harmonic peaks, certain prerequisite conditions must be met. Specifically, the harmonic peaks must be resolved and arise from the interference of only two attosecond bursts [45]. This resolution depends on the temporal profile of the laser electric field, which is influenced by two critical parameters: pulse duration (i.e., the number of optical cycles) and the carrier-envelope phase (CEP) (i.e., the phase difference between the pulse envelope and the carrier wave). How these parameters affect the observability of the MEP-induced frequency shift of HHG peaks in CO molecules remains an open question. In Ref. [45], by initial estimations, we stated that the CEP should not be close to  $\pi/2$  and  $3\pi/2$ , and that the pulse duration should lie between 3 and 6 cycles. However, the specific ranges of these laser parameters and how they affect the peak resolution have not been discussed. Moreover, in our previous investigation of frequency shift induced by the addition of a static electric field to the laser–atom system, we demonstrated that such frequency shifts are observable only for CEP values within a specific range [47]. Whether this CEP range is still applicable for observing MEP-induced peak shifts in CO is yet to be further investigated.

In this paper, we identify the ranges of pulse duration and CEP that are optimal for observing the frequency shift induced by MEP when the CO molecule interacts with few-cycle laser pulses. The physical mechanisms underlying how these parameters influence the harmonic peaks are also discussed. To compute the HHG spectra, we numerically solve the time-dependent Schrödinger equation (TDSE).

#### 2. Physical mechanism of MEP-induced frequency shift and method for calculating HHG

In this section, we first explain the mechanism behind the frequency shift induced by MEP in HHG spectra when a polar molecule interacts with a few-cycle laser pulse. Then, we outline the numerical method utilized to calculate the HHG spectra of the CO molecule, taking into account the MEP effect.

#### 2.1. Mechanism of MEP-induced frequency shift of harmonic peaks

The mechanism of the frequency shift of HHG peaks in the cutoff region, induced by variations in asymmetry factors of targets interacting with few-cycle laser pulses, has been thoroughly discussed in previous works [39,45]. Below, we briefly outline the fundamental principles and the relevant equations.

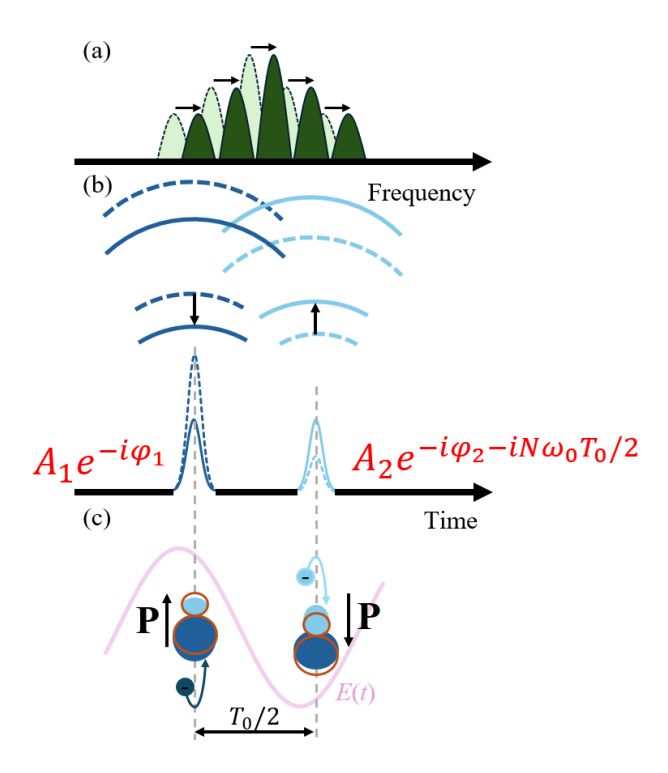


**Fig. 1.** Mechanism of frequency shift induced by MEP (denoted as P). MEP alters the shape of the molecular orbital (c), thereby modifying both the intensity and phase of the two attosecond bursts emitted half a cycle apart (b), which ultimately leads to a shift in the HHG spectral peak (a).

In Fig. 1, we sketch the mechanism of the MEP-induced frequency shift of harmonic peaks in the cutoff region of HHG spectra. When a laser pulse interacts with a CO molecule, the process begins when the electric field reaches its peak, causing an electron to be freed from the molecule through tunnel ionization. Once liberated, the electron is driven by the laser's electric field and then backward to recombine with the parent ion, emitting a high-harmonic pulse known as an

attosecond burst. After half a laser cycle, the electric field reverses direction, pulling the electron out again near its peak and driving it back to recombine at the opposite end of the molecule, generating the next attosecond burst [Fig. 1(c)]. In the case of a few-cycle laser pulse, only two dominant attosecond bursts, denoted as  $A_1e^{-i\varphi_1}$  and  $A_2e^{-i\varphi_2-iN\omega_0T_0/2}$ , contribute to the HHG at the cutoff region, as illustrated in Fig. 1(b). Here,  $A_1$  and  $A_2$  represent the amplitudes, while  $\varphi_1$  and  $\varphi_2$  are the phases of the two attosecond bursts, N denotes the harmonic order, and  $\omega_0$  and  $T_0$  are the laser frequency and period, respectively. The interference between these two attosecond bursts forms spectral peaks, as shown in Fig. 1(a), at the harmonic order

$$N = 2k + 1 + \frac{\Delta \varphi}{\pi}.\tag{1}$$

Here, k is an integer, and  $\Delta \varphi = \varphi_1 - \varphi_2$  represents the phase difference between the two attosecond bursts. For a few-cycle laser pulse, the HHG peak may occur at positions that do not correspond to odd integer harmonic orders. The interference of the two attosecond bursts resembles the two-center interference in classical physics.

When MEP is included, the laser-induced polarization of the core electrons leads to the distortion of the molecular orbital, thereby altering both the amplitude and phase of the attosecond bursts, as shown in Figs. 1[(b), (c)]. As a consequence, the interference pattern [Fig. 1(a)] updates the harmonic peaks at the new order

$$N' = 2k + 1 + \frac{\Delta \varphi'}{\pi}.\tag{2}$$

Here,  $\Delta \phi' = \phi_1' - \phi_2'$  denotes the phase difference between the two attosecond bursts when MEP is included. Therefore, when comparing the cases with and without the MEP effect, the HHG peak is shifted by an amount (in harmonic order) given by

$$\Delta N = \frac{\delta \Delta \varphi}{\pi},\tag{3}$$

with  $\delta\Delta\phi=\Delta\phi'-\Delta\phi$  represents the distortion of the phase difference induced by MEP. Thus, the underlying origin of the MEP-induced frequency shift of harmonic peaks is the MEP-induced changes in the phases of attosecond bursts. To observe a clear frequency shift, the condition is that only two attosecond bursts interfere with each other. If a third burst evolves, the interference pattern becomes more complex, making identifying and quantifying the peak shift significantly more challenging.

# 2.2. Method for numerically calculating HHG

We briefly present the numerical method for solving TDSE to calculate HHG. Detailed descriptions of the method can be found in Ref. [28]. In atomic units ( $\hbar = m_e = e = 1$ ), the interaction between the molecule and the laser field is described by the TDSE as

$$i\frac{\partial}{\partial t}\psi(\mathbf{r},t) = \left(-\frac{\nabla^2}{2} + V_{SAE}(\mathbf{r}) + \mathbf{r} \cdot \mathbf{E}(t)\right)\psi(\mathbf{r},t),\tag{4}$$

where  $\mathbf{r}$  denotes the position vector of the electron. The potential  $V_{SAE}$  of the CO molecule is constructed based on the single active-electron (SAE) model [48, 49]. In this model, only the outermost electron is allowed to interact with the laser field, while the remaining electrons are assumed to be frozen and move together with the nuclei. This approach yields the energy and dipole

moment of the highest occupied molecular orbital (HOMO) of the CO molecule as -0.515 a.u. and 1.57 a.u., respectively.

The laser field has the form

$$\mathbf{E}(t) = \mathbf{e}E_0 \sin^2\left(\frac{\omega_0 t}{2N_{oc}}\right) \sin(\omega_0 t + \phi), \tag{5}$$

where  $E_0$ ,  $\omega_0$ ,  $\phi$ , and  $N_{oc}$  respectively denote the peak amplitude, carrier frequency, carrier-envelope phase (CEP), and number of optical cycles of the laser pulse. In this work, the laser polarization is oriented such that the unit vector  $\mathbf{e}$  is directed from the C atom toward the O atom. The molecular axis of the CO molecule is aligned along the *z*-axis.

To investigate the influence of MEP on the HHG spectra, we include an additional polarization potential term [20], which takes the form

$$V_{\rm P}(\mathbf{r},t) = -\frac{\mathbf{E}(t)\hat{\boldsymbol{\alpha}}_c \cdot \mathbf{r}}{r^3}.$$
 (6)

Here,  $\hat{\alpha}_c$  is the polarizability tensor of the CO<sup>+</sup> cation, with its components given as  $\alpha_{cxx} = \alpha_{cyy} = 6.72$  a.u. and  $\alpha_{czz} = 12.2$  a.u. [50].

To solve Eq. (4), the time-dependent wavefunction  $\psi(\mathbf{r},t)$  is expanded in terms of time-independent basis functions  $\psi(\mathbf{r},t=0)$ . These initial wavefunctions are constructed by expanding into B-spline functions in the radial coordinate and spherical harmonics in the angular coordinates. The expansion time-dependent coefficients  $\psi(\mathbf{r},t)$  are then solved by the fourth-order Runge-Kutta method. The computational parameters are chosen to be the same as those used in Ref. [32] to ensure the convergence of the results.

After obtaining the time-dependent wavefunction  $\psi(\mathbf{r},t)$ , we compute the induced dipole acceleration using the expression  $\mathbf{a}(t) = \frac{d^2}{dt^2} \langle \psi(\mathbf{r},t) | \mathbf{r} | \psi(\mathbf{r},t) \rangle$ . The HHG intensity is then calculated via the Fourier transform of the dipole acceleration

$$S(N\omega_0) \propto \left| \int_0^{N_{oc}T_0} a(t)e^{iN\omega_0 t} dt \right|^2.$$
 (7)

To extract how HHG emits with time (i.e., attosecond burst), we compute the harmonic time-frequency profile by applying the Gabor transform, defined as

$$S(N\omega_0, t) \propto \left| \int dt' a(t') \frac{\exp\left[-(t'-t)^2/2\sigma^2\right]}{\sigma\sqrt{2\pi}} e^{iN\omega_0 t} \right|^2,$$
 (8)

where  $\sigma = (3\omega_0)^{-1}$  is the window width, chosen to balance between temporal and spectral resolutions.

#### 3. Result and discussion

In this section, we present the results of the observability of the HHG frequency shift induced by MEP under variations of the laser CEP and pulse duration. We do not examine the influence of laser intensity and wavelength, as these two parameters do not affect the number of contributing attosecond bursts and, therefore, do not affect the observability of the harmonic

shift [45]. Throughout this section, the laser intensity is fixed at  $1.5 \times 10^{14}$  W/cm<sup>2</sup>, and the wavelength is set to 800 nm. The electric field of the laser is polarized parallel to the molecular axis, with the unit vector  $\mathbf{e}$  directed from the C atom to the O atom.

# 3.1. Optimal CEP range for observing MEP-induced frequency shift

# 3.1.1. Optimal CEP range

In Fig. 2, we present the HHG spectra in the cutoff region for the CO molecule, comparing two cases: one with the inclusion of MEP (denoted as SAE+P) and one without (denoted as SAE), for various values of laser CEP. The laser pulse duration is set to five optical cycles. The results in Fig. 2(d) show that when  $\phi = \pi$ , the HHG peaks in the presence of MEP (SAE+P) shift to the left (a redshift) by approximately 0.8 harmonic orders compared to the case without MEP (SAE). Conversely, when  $\phi = 0$ , the spectral peaks with MEP shift to the right (a blueshift) by about 0.8 harmonic orders, as shown in Fig. 2(j). In our previous work [45], we demonstrated that this frequency shift is a universal characteristic for each harmonic energy and remains nearly unchanged when changing the laser intensity and wavelength.

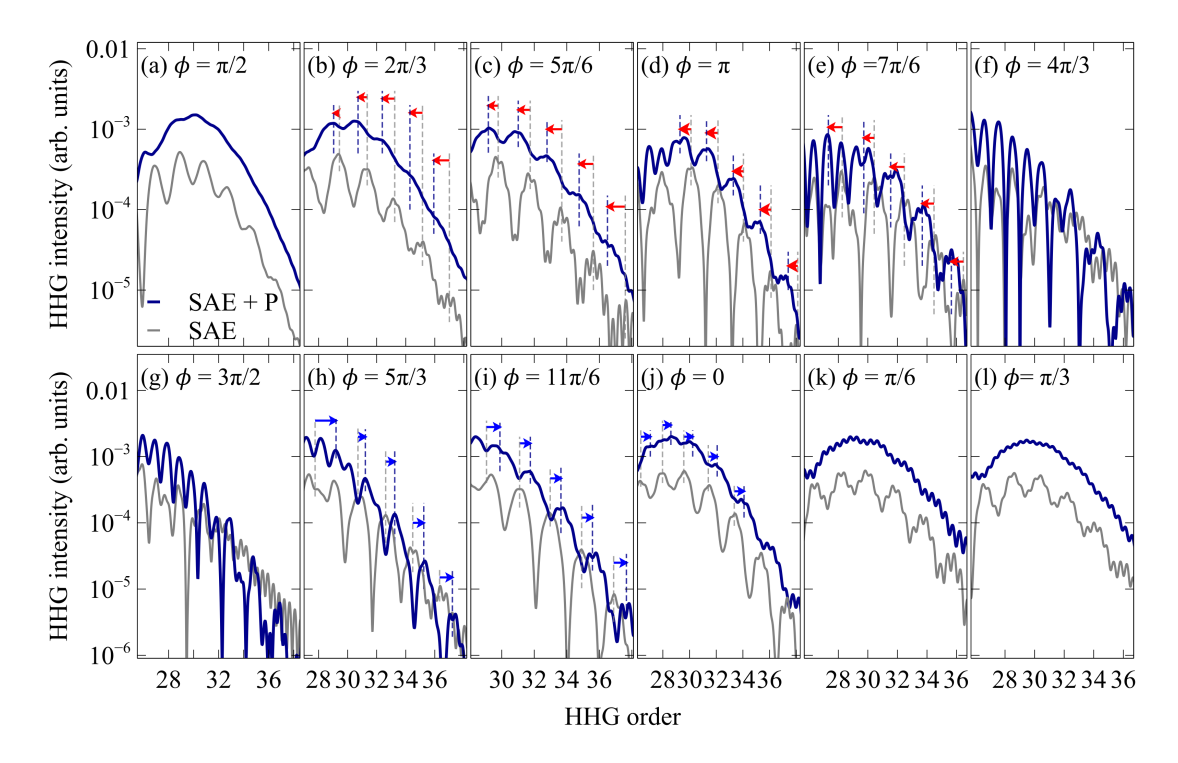


**Fig. 2.** MEP-induced frequency shift of harmonic peaks at the cutoff region of the CO molecule when including MEP (denoted as SAE+P) and ignoring MEP (denoted as SAE), when varying the CEP of the laser pulse. The short vertical dashed lines mark the peak positions of harmonics. The red and blue arrows exhibit the redshifts and blueshifts of harmonic peaks when considering MEP compared to those ignoring MEP. The laser pulse has a duration of five optical cycles, an intensity of  $1.5 \times 10^{14}$  W/cm<sup>2</sup>, and a wavelength of 800 nm.

Figure 2 also shows that the frequency shift is most pronounced when the CEP is  $\pi$  or  $11\pi/6$ . As the CEP decreases from  $\pi$  downward  $\pi/2$ , as shown in Figs. 2[(a)–(d)], or increases from 0 to  $\pi/2$ , as illustrated in Figs. 2[(j)–(l)], the harmonic peaks at higher orders (specifically near the end of the cutoff region) gradually diminish, especially when MEP is included. The frequency shift is more pronounced for lower-energy harmonic peaks at the beginning of the cutoff region compared to those at the end. Additionally, the rule governing the magnitude of the shift becomes more complex across the cutoff region. When the CEP approaches  $\pi/2$ , the HHG peaks become unresolved, making it impossible to detect the MEP-induced spectral shift. Conversely, as the CEP increases from  $\pi$  to  $3\pi/2$ , as shown in Figs. 2[(d)–(g)], or decreases from  $2\pi$  (which is equivalent to 0) to  $3\pi/2$ , as illustrated in Figs. 2[(g)–(j)], the harmonic peaks exhibit more complex structures where each peak splits into multiple sub-peaks. This complicates the identification of the HHG peak positions and obscures the observation of the MEP-induced peaks' shift.

In short, after scanning the laser CEP, we conclude that the MEP-induced frequency shift of harmonic peaks at the cutoff region is most clearly observed when the CEP is within the ranges of  $(2\pi/3, 7\pi/6)$  and  $(5\pi/3, 2\pi)$ , that is, in the vicinity of 0 and  $\pi$ . This CEP range is significantly narrower than that required to observe frequency shift induced by adding a static electric field to the laser–atom system [43, 47]. The reason is that MEP affects not only the phase but also the intensity of attosecond bursts, leading to reduced spectral peak resolution [45]. It is evident that in Fig. 2, the peak resolution with MEP is considerably worse than that without it for most laser CEP values. In contrast, a weak static field mainly influences the phase of attosecond bursts without significantly degrading the resolution of HHG peaks [43, 47].

#### 3.1.2. Explanation by the interference pictures

To explain the origin of the observations mentioned above, we examine the interference pattern of attosecond bursts. In Figs. 3[(a1)-(11)], we present the time-frequency profile of HHG from the CO molecule with considering the MEP, for different values of CEP. The horizontal grey dashed lines indicate the 30th harmonic (H30), corresponding to the cutoff of the HHG spectra. The results show that for CEP values around 0 or  $\pi$ , the HHG peaks in the cutoff region are formed by the interference of two attosecond bursts emitted near instants  $2.3T_0$  and  $2.8T_0$ . These two bursts have comparable maxima in harmonic orders. As a result, their interference creates well-resolved peaks for harmonics in the cutoff region. Furthermore, the MEP alters the relative phase between the two attosecond bursts, which shifts the position of the HHG peaks compared to the scenario without MEP. This is illustrated in Figs. 2[(d), (j)].

For CEP closes to  $\pi/2$ , the time-frequency profile shown in Fig. 3(a) reveals a distinct difference in the maximum orders among the attosecond bursts. The cutoff region is predominantly formed by a single attosecond burst emitted around  $2.5T_0$ , without contributions from other bursts. The absence of interference between multiple attosecond bursts results in a smooth HHG spectrum in the cutoff region, which does not exhibit well-resolved spectral peaks.

As the CEP decreases from  $\pi$  to  $\pi/2$ , or increases from 0 to  $\pi/2$ , the difference in maximum orders between the two attosecond bursts progressively increases, as shown in Figs. 3[(a)–(d), (j)–(l)]. Consequently, the HHG peaks become less resolved and gradually evolve into a smoother spectrum, as shown in Figs. 2[(a)–(d), (j)–(l)]. In contrast, when the CEP increases from  $\pi$  to  $3\pi/2$ , or decreases from  $2\pi$  (i.e., 0) to  $3\pi/2$ , three attosecond bursts emerge with comparable maximum harmonic orders, as illustrated in Figs. 3[(d)–(g), (g)–(j)]. Consequently, all three bursts

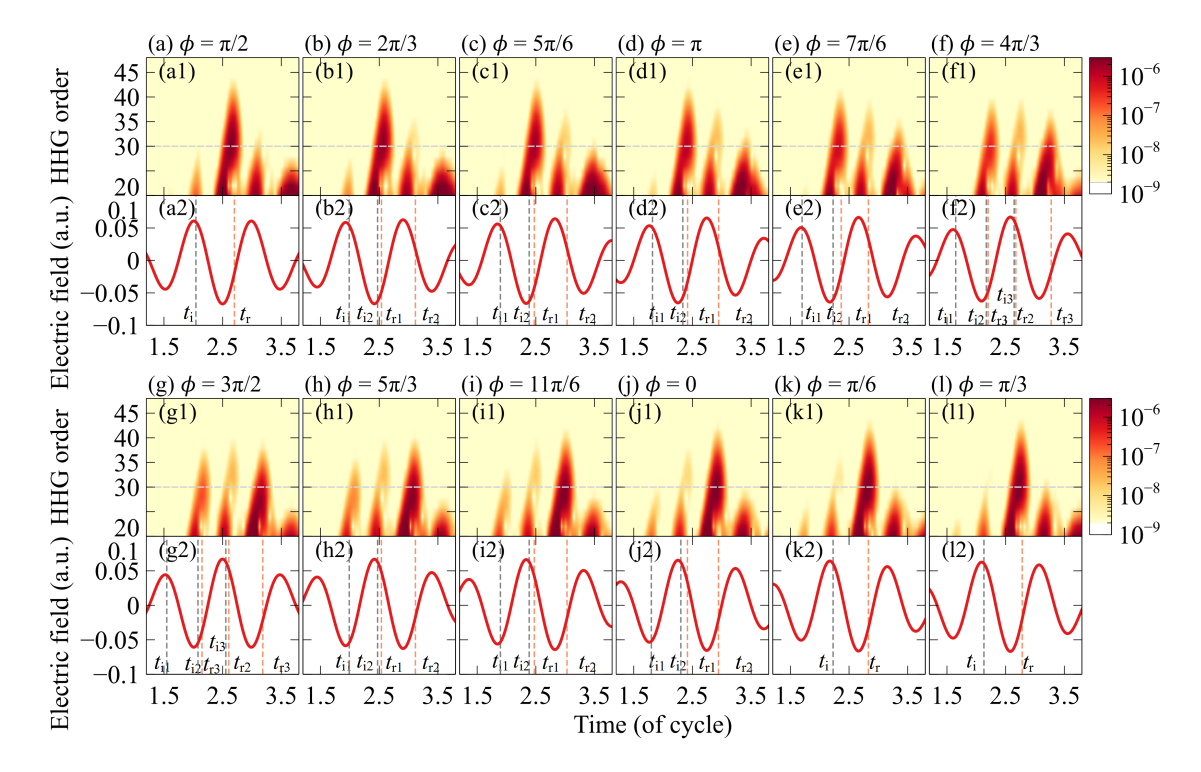


**Fig. 3.** Time-frequency profile of the HHG spectra of the CO molecule with the inclusion of the MEP effect (first and third rows). The horizontal grey dashed line indicates the 30th harmonic (H30). The color bar encodes the intensity of attosecond bursts. The second and fourth rows depict the corresponding temporal profiles of the laser pulses with different CEPs. The vertical dashed lines mark the ionization instants  $t_i$  (in black) and recombination instants  $t_r$  (in orange) responsible for the attosecond bursts contributing to harmonics in the cutoff region. The laser parameters used are the same as those in Fig. 2.

contribute to the harmonics within the cutoff region. This results in a more complex interference pattern, which leads to irregular peak shifts and the splitting of peaks into sub-peaks for harmonics in the cutoff region, as displayed in Figs. 2[(a)-(d), (j)-(l)]. Thus, it becomes significantly more challenging to clearly identify the spectral peak shifts induced by MEP.

#### 3.1.3. Origin of interference pictures

To gain further insight into the behavior of the time-frequency profiles while varying laser CEP, we also display the corresponding temporal profiles of the laser pulse in Figs. 3[(a2)-(l2)]. In these figures, we also enclose the ionization and recombination instants of the liberated electrons, which are responsible for the emission of the attosecond bursts. These instants are obtained by solving the classical motion of liberated electrons in the laser electric field [4, 5].

Figures 3[(d2),(j2)] show that for CEP of 0 or  $\pi$ , the two central half-cycles of the laser pulse exhibit comparable peak field strengths. Consequently, the electric field amplitudes in the intervals  $(t_{i1}, t_{r1})$  and  $(t_{i2}, t_{r2})$  are nearly the same. The electrons propagating during these intervals acquire similar kinetic energies, and upon recombination, they generate two attosecond

bursts with comparable maximum harmonic orders, as shown in Figs. 3[(d1),(j1)]. In contrast, for the case where  $\phi = \pi/2$ , as exhibited in Fig. 3(a2), only one central half-cycle reaches the maximum field strength, resulting in the highest kinetic energy for the electron. Additionally, MEP enhances the intensity of an attosecond burst emitted at the central pulse while diminishing the strength of the adjacent bursts [21, 32, 45, 51]. This leads to a single dominant attosecond burst that significantly contributes to the harmonic cutoff region, as shown in Fig. 3(a1).

When the CEP increases from  $\pi$  to  $3\pi/2$ , or decreases from  $2\pi$  (or 0) to  $3\pi/2$ , the electric field changes in such a way that three half-cycles with comparable amplitudes appear as demonstrated in Figs. 3[(d2)-(f2),(g2)-(j2)]. This results in three attosecond bursts with similar maximum harmonic orders, leading to three-burst interference for harmonics at the cutoff. At CEP of  $3\pi/2$  shown in Fig. 3(g2), the central half-cycle of the laser pulse reaches its maximum field strength, similar to what occurs at  $\phi = \pi/2$ . However, because the MEP reduces the intensity of the central attosecond burst while enhancing the two neighboring bursts, all three attosecond bursts contribute to generating harmonics in the cutoff region, as indicated in Fig. 3(g1).

# 3.2. Optimal pulse durations for observing MEP-induced frequency shift

# 3.2.1. Optimal pulse durations

We further investigate the observability of the frequency shift as a function of laser pulse duration. In Figs. 4[(a1)–(d1)], we present the cutoff region of the HHG spectra emitted from the CO molecule under interaction with laser pulses of varying numbers of optical cycles, comparing the cases with and without the inclusion of the MEP effect.

Figures 4[(a1), (c1)] show that the spectral peak shift is clearly and consistently observed in the cutoff region when the laser pulse duration is three or five optical cycles. In these cases, the cutoff region is created by the interference of two attosecond bursts, as shown in Figs. 4[(a2), (c2)]. These bursts are emitted during the recombination of electrons that are liberated from both sides of CO molecules at two different ionization instants, as marked in Figs. 4[(a3), (c3)]. Consequently, using three-cycle and five-cycle pulses is suitable for observing the MEP-induced frequency shift.

When the pulse duration is four optical cycles, and the CEP is fixed at  $\pi$ , although the HHG spectrum without MEP still exhibits well-defined peaks, the spectrum becomes smooth when MEP is included, as shown in Fig. 4(b1). This smoothing occurs because MEP suppresses the intensity of the first attosecond burst while enhancing the second burst [45]. Consequently, the cutoff region is dominated by a single attosecond burst, as illustrated in Fig. 4(b2). In contrast, when the CEP is adjusted to 0 while maintaining the same four-cycle pulse, the frequency shift becomes clearly observable again (not shown). In this case, MEP enhances the intensity of the first attosecond burst and reduces the intensity of the second burst, resulting in two bursts of comparable intensity [45]. It is important to note that laser pulses shorter than three optical cycles are unsuitable for observing the frequency shift induced by MEP. These shorter pulses typically generate only a single dominant attosecond burst, which leads to smooth HHG spectra without well-defined peaks, thus preventing the observation of frequency shifts.

As the number of optical cycles increases to six, seven, and eight, as demonstrated in Figs. 4[(d1)-(f1)], the frequency shifts remain observable. However, these shifts become less stable and more irregular, with peaks accompanied by the emergence of secondary peaks. The complex peak structure in the cutoff region results from the interference of multiple attosecond

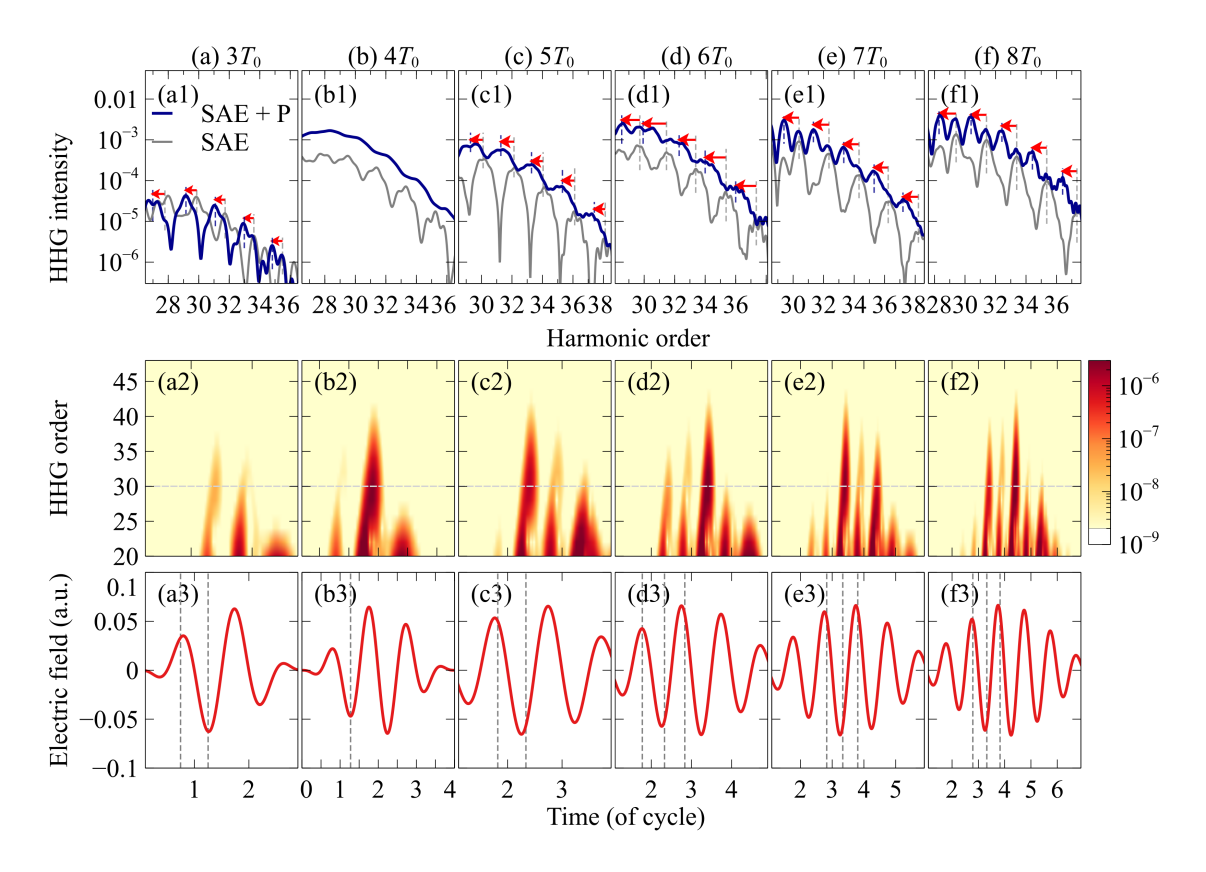


**Fig. 4.** Cutoff region of the HHG spectra with (SAE+P) and without (SAE), including the MEP effect for laser pulses with varying numbers of optical cycles (top panels). The red arrows indicate the redshift of harmonic peaks. The middle panels show the corresponding time-frequency profile of HHG where the MEP is included. The bottom panels display the temporal profiles of laser electric fields for different pulse durations, with vertical dashed lines marking the ionization moments responsible for the emission of attosecond bursts. The electric field has an intensity of  $1.5 \times 10^{14}$  W/cm<sup>2</sup>, a wavelength of 800 nm, and a CEP of  $\pi$ .

bursts, as illustrated in Figs. 4[(d2)–(f2)]. This phenomenon occurs because, as the pulse duration increases, the difference in electric field intensity between successive half-cycles diminishes, as presented in Figs. 4[(d3)–(f3)]. Consequently, more attosecond bursts with more comparable maximum harmonic orders contribute to generating harmonics in the cutoff region. In these cases, besides the interference from two adjacent attosecond bursts (known as sub-cycle interference) that causes the harmonic shift, there is also inter-cycle interference from bursts that are spaced one optical cycle apart [39, 43]. This inter-cycle interference is responsible for the generation of odd and even harmonics [39]. The combination of both sub-cycle and inter-cycle interferences complicates the spectral patterns, as shown in Figs. 4[(d1)-(f1)]. Furthermore, in these regimes, the frequency shift is not solely induced by MEP but is also influenced by variations in the electric

field across different half-cycles [45]. As a result, using these laser pulses makes it challenging to isolate the MEP-induced shift of the harmonic peaks.

Therefore, we conclude that, to clearly and purely observe the MEP-induced frequency shift in the HHG cutoff region, the laser pulse duration should be greater than three and less than six optical cycles.

# 3.2.2. Transition from MEP-induced peaks' frequency shift to MEP-induced odd-even intensity modification

We further increase the number of optical cycles, as shown in Figs. 5[(a)-(c)]. The results reveal a clear transition from MEP-induced frequency shift to modulation in the intensity of even-odd peaks as the pulse duration increases from a few-cycle [Fig. 5(a)] to multi-cycle [Fig. 5(c)]. For laser pulses of moderate duration, Fig. 5(b) shows that the frequency shift remains observable, though the magnitude of the shift is relatively small.

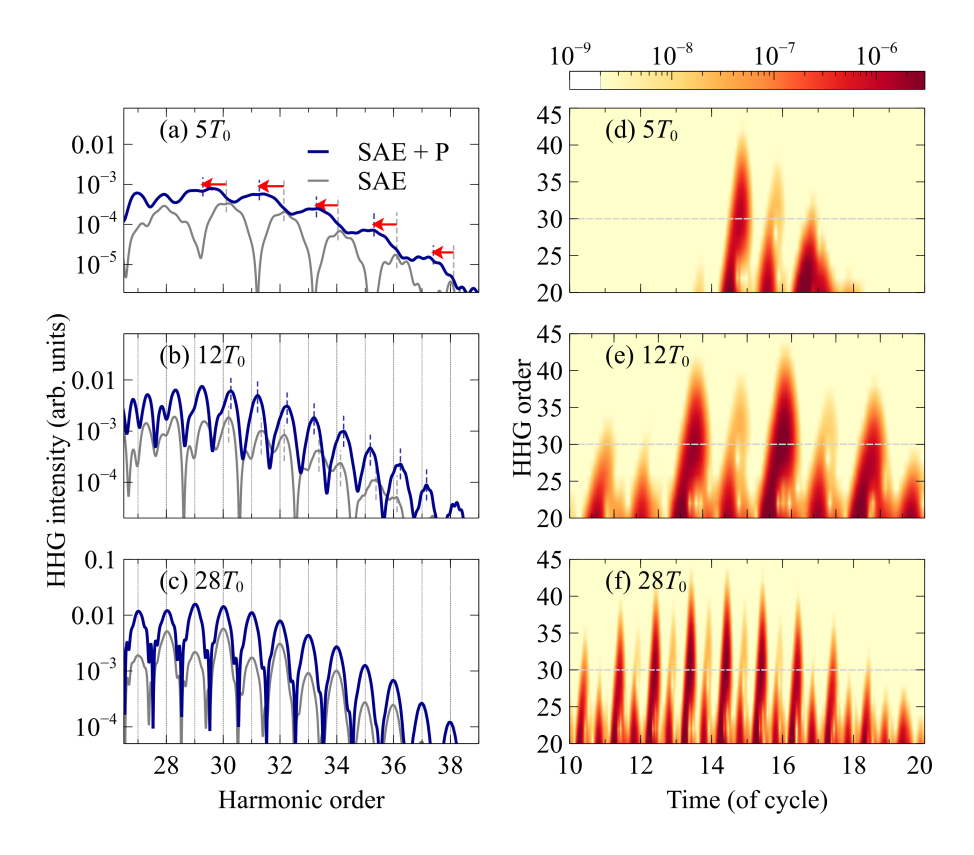


**Fig. 5.** Transition from MEP-induced frequency shift when using a few-cycle laser pulse (a) to the modification of the intensity of odd-even peak using a multi-cycle pulse (c). For intermediate pulse durations, both the spectral shift and the variation in peak intensity occur simultaneously (b). The corresponding time-frequency profiles with MEP included are shown in the right panels. The laser parameters are identical to those used in Fig. 4.

The above-mentioned behavior can be understood by examining the corresponding time-frequency profiles in Figs. 5[(d)–(f)]. As the pulse duration increases, we observe a transition from sub-cycle interference, which occurs when only two attosecond bursts are emitted, to intercycle interference, which involves the repeated interference of pairs of attosecond bursts across multiple optical cycles. When using multi-cycle laser pulses, inter-cycle interference constrains the harmonics to fixed even and odd orders, while sub-cycle interference influences their relative intensities [39]. Since MEP primarily influences the amplitude and phase of attosecond burst pairs, it modulates sub-cycle interference, causing variations in the intensity of odd and even orders when multi-cycle laser pulses are used. When using intermediate pulses, intercycle interference is not yet prominent compared to sub-cycle interference. As a result, the positions of the harmonic peaks may not arise in odd and even orders. Therefore, both frequency shifts and peak intensities are induced by MEP. In contrast, when employing a few-cycle pulse, pure sub-cycle interference causes clean MEP-induced frequency shifts of harmonic peaks at the cutoff region.

This transition from MEP-induced harmonic peaks' frequency shift to MEP-induced oddeven intensity variation while increasing laser pulse duration aligns with observations made in other systems influenced by various factors that induce asymmetry, such as static electric fields, the degree of asymmetry between two atoms in a heteronuclear molecule, or the orientation angle between the laser polarization and the molecular axis [39].

# 4. Conclusions

In this paper, we have investigated the optimal ranges of laser CEP and pulse durations for observing the HHG spectral peak shift induced by the MEP effect in the CO molecule interacting with intense, ultrashort laser pulses. We demonstrated that the fundamental mechanism causing the frequency shift is the MEP-induced modification of the sub-cycle interference pattern between two attosecond bursts. Therefore, a key condition for observing the MEP-induced spectral shift is that the temporal profiles of the laser pulses must be suitable for generating only two attosecond bursts.

By employing the theoretical approach based on solving TDSE for the laser–CO molecule system, we have identified the optimal parameter ranges for observing the MEP-induced frequency shift. Specifically, we have found that CEP should fall within the ranges of  $(2\pi/3, 7\pi/6)$  and  $(5\pi/3, 2\pi)$ . Additionally, the pulse duration must be greater than three and less than six optical cycles to purely observe the MEP-induced frequency shift. These optimal regions are important for guiding experiments in selecting the appropriate laser to directly observe the effect of core electrons on the HHG spectrum through peak shifts.

## Acknowledgements

This research was funded by Vietnam National Foundation for Science and Technology Development under Grant No. 103.01-2021.28. This work was carried out by the high-performance computing cluster at Ho Chi Minh City University of Education, Vietnam.

## **Conflict of interest**

The authors have no conflict of interest to declare.

# References

- [1] T. Brabec and F. Krausz, *Intense few-cycle laser fields: Frontiers of nonlinear optics*, Rev. Mod. Phys. **72** (2000) 545.
- [2] P. Peng, C. Marceau and D. M. Villeneuve, Attosecond imaging of molecules using high harmonic spectroscopy, Nat. Rev. Phys. 1 (2019) 144.
- [3] F. Krausz and M. Ivanov, Attosecond physics, Rev. Mod. Phys. 81 (2009) 163.
- [4] P. B. Corkum, Plasma perspective on strong field multiphoton ionization, Phys. Rev. Lett. 71 (1993) 1994.
- [5] M. Lewenstein, P. Balcou, M. Y. Ivanov, A. L'Huillier and P. B. Corkum, Theory of high-harmonic generation by low-frequency laser fields, Phys. Rev. A 49 (1994) 2117.
- [6] T. Popmintchev, M.-C. Chen, D. Popmintchev, P. Arpin, S. Brown, S. Ališauskas et al., Bright coherent ultrahigh harmonics in the keV X-ray regime from mid-infrared femtosecond lasers, Science 336 (2012) 1287.
- [7] M. Chergui, M. Beye, S. Mukamel, C. Svetina and C. Masciovecchio, *Progress and prospects in nonlinear extreme-ultraviolet and X-ray optics and spectroscopy*, Nat. Rev. Phys. **5** (2023) 578.
- [8] M. Hentschel, R. Kienberger, C. Spielmann, G. A. Reider, N. Milosevic, T. Brabec et al., Attosecond metrology, Nature 414 (2001) 509.
- [9] M. Lein, N. Hay, R. Velotta, J. P. Marangos and P. L. Knight, *Interference effects in high-order harmonic generation with molecules*, Phys. Rev. A **66** (2002) 023805.
- [10] O. Smirnova, Y. Mairesse, S. Patchkovskii, N. Dudovich, D. Villeneuve, P. Corkum et al., High harmonic interferometry of multi-electron dynamics in molecules, Nature 460 (2009) 972.
- [11] S. Pabst and R. Santra, Strong-field many-body physics and the giant enhancement in the high-harmonic spectrum of xenon, Phys. Rev. Lett. 111 (2013) 233005.
- [12] P. Kraus, O. I. Tolstikhin, D. Baykusheva, A. Rupenyan, J. Schneider, C. Z. Bisgaard et al., Observation of laser-induced electronic structure in oriented polyatomic molecules, Nat. Commun. 6 (2015) 7039.
- [13] L. He, Q. Zhang, P. Lan, W. Cao, X. Zhu, C. Zhai et al., Monitoring ultrafast vibrational dynamics of isotopic molecules with frequency modulation of high-order harmonics, Nat. Commun. 9 (2018) 1108.
- [14] L. Li, Y. Zhang, P. Lan, T. Huang, X. Zhu, C. Zhai et al., Dynamic core polarization in high harmonic generation from solids: The example of MgO crystals, Phys. Rev. Lett. 126 (2021) 187401.
- [15] K. Amini, J. Biegert, F. Calegari, A. Chacón, M. F. Ciappina, A. Dauphin et al., Symphony on strong field approximation, Rep. Prog. Phys. 82 (2019) 116001.
- [16] M. Ammosov, N. Delone and V. Krainov, *Tunnel ionization of complex atoms and of atomic ions in an alternating electromagnetic field*, J. Exp. Theor. Phys. **64** (1986) 1191.
- [17] S. Pabst, L. Greenman, D. A. Mazziotti and R. Santra, Impact of multichannel and multipole effects on the cooper minimum in the high-order-harmonic spectrum of argon, Phys. Rev. A 85 (2012) 023411.
- [18] J. Wu, L. P. H. Schmidt, M. Kunitski, M. Meckel, S. Voss, H. Sann et al., Multiorbital tunneling ionization of the CO molecule, Phys. Rev. Lett. 108 (2012) 183001.
- [19] E. Frumker, N. Kajumba, J. B. Bertrand, H. J. Wörner, C. T. Hebeisen, P. Hockett et al., Probing polar molecules with high harmonic spectroscopy, Phys. Rev. Lett. 109 (2012) 233904.
- [20] Z. Zhao and T. Brabec, Tunnel ionization in complex systems, J. Mod. Opt. 54 (2007) 981.
- [21] B. Zhang, J. Yuan and Z. Zhao, Dynamic core polarization in strong-field ionization of CO molecules, Phys. Rev. Lett. 111 (2013) 163001.
- [22] M. Abu-samha and L. B. Madsen, Multielectron effects in strong-field ionization of the oriented OCS molecule, Phys. Rev. A 102 (2020) 063111.
- [23] M. Abu-samha and L. B. Madsen, Effect of multielectron polarization in the strong-field ionization of the oriented CO molecule, Phys. Rev. A 101 (2020) 013433.
- [24] M. Abu-samha, L. B. Madsen and N. I. Shvetsov-Shilovski, Multielectron effect in strong-field ionization of CO, 2024.
- [25] D. Dimitrovski, J. Maurer, H. Stapelfeldt and L. B. Madsen, Low-energy photoelectrons in strong-field ionization by laser pulses with large ellipticity, Phys. Rev. Lett. 113 (2014) 103005.
- [26] A. A. Romanov, A. A. Silaev, M. V. Frolov and N. V. Vvedenskii, Influence of the polarization of a multielectron atom in a strong laser field on high-order harmonic generation, Phys. Rev. A 101 (2020) 013435.

- [27] B. Zhang, J. Yuan and Z. Zhao, Dynamic orbitals in high-order harmonic generation from CO molecules, Phys. Rev. A 90 (2014) 035402.
- [28] C.-T. Le, V.-H. Hoang, L.-P. Tran and V.-H. Le, Effect of the dynamic core-electron polarization of CO molecules on high-order harmonic generation, Phys. Rev. A 97 (2018) 043405.
- [29] C.-T. Le, D.-D. Vu, C. Ngo and V.-H. Le, Influence of dynamic core-electron polarization on the structural minimum in high-order harmonics of CO<sub>2</sub> molecules, Phys. Rev. A **100** (2019) 053418.
- [30] C.-T. Le, C. Ngo, N.-L. Phan, D. Vu and V.-H. Le, Dynamic core-electron-polarization effect on the high-order harmonic generation process from a quantum-trajectory perspective, Phys. Rev. A 107 (2023) 043103.
- [31] C.-T. Le, N.-L. Phan and V.-H. Le, *Electron dynamical phase difference and high-order harmonic frequency shift: A Bohmian-trajectory perspective*, Phys. Rev. A **110** (2024) 063115.
- [32] H. T. Nguyen, K.-N. H. Nguyen, N.-L. Phan, C.-T. Le, D. Vu, L.-P. Tran et al., Imprints of multielectron polarization effects in odd-even harmonic generation from CO molecules, Phys. Rev. A 105 (2022) 023106.
- [33] N.-L. Phan, C.-T. Le, V.-H. Hoang and V.-H. Le, *Odd–even harmonic generation from oriented CO molecules in linearly polarized laser fields and the influence of the dynamic core-electron polarization*, Phys. Chem. Chem. Phys. **21** (2019) 24177.
- [34] N. Ben-Tal, N. Moiseyev and A. Beswick, The effect of hamiltonian symmetry on generation of odd and even harmonics, J. Phys. B: At. Mol. Opt. Phys. 26 (1993) 3017.
- [35] O. Neufeld, D. Podolsky and O. Cohen, Floquet group theory and its application to selection rules in harmonic generation, Nat. Commun. 10 (2019) 405.
- [36] C.-T. Le, N.-L. Phan, D. D. Vu, C. Ngo and V.-H. Le, Effect of multiple rescatterings on continuum harmonics from asymmetric molecules in multicycle lasers, Phys. Chem. Chem. Phys. 24 (2022) 6053.
- [37] K.-N. H. Nguyen, N.-L. Phan, C.-T. Le, D. Vu and V.-H. Le, Parameter-free retrieval of subcycle asymmetry of polar molecules by high-order harmonic spectroscopy, Phys. Rev. A 106 (2022) 063108.
- [38] D.-A. Trieu, N.-L. Phan, Q.-H. Truong, H. T. Nguyen, C.-T. Le, D. Vu et al., Universality in odd-even harmonic generation and application in terahertz waveform sampling, Phys. Rev. A 108 (2023) 023109.
- [39] D.-A. Trieu, V.-H. Le and N.-L. Phan, Laser-target symmetry breaking in high-order harmonic generation: From frequency shift to odd-even intensity modulation, Phys. Rev. A 110 (2024) L041101.
- [40] D. Shafir, Y. Mairesse, D. Villeneuve, P. Corkum and N. Dudovich, *Atomic wavefunctions probed through strong-field light–matter interaction*, Nat. Physics **5** (2009) 412.
- [41] Y. Chen and B. Zhang, *Tracing the structure of asymmetric molecules from high-order harmonic generation*, Phys. Rev. A **84** (2011) 053402.
- [42] A. Y. Naumov, D. Villeneuve and H. Niikura, Contribution of multiple electron trajectories to high-harmonic generation in the few-cycle regime, Phys. Rev. A 91 (2015) 063421.
- [43] D.-A. Trieu, T.-T. D. Nguyen, T.-D. D. Nguyen, T. Tran, V.-H. Le and N.-L. Phan, *Analytically controlling the laser-induced electron phase in sub-cycle motion*, Phys. Rev. A **110** (2024) L021101.
- [44] Y. S. You, Y. Yin, Y. Wu, A. Chew, X. Ren, F. Zhuang et al., High-harmonic generation in amorphous solids, Nat. Commun. 8 (2017) 724.
- [45] K.-N. H. Nguyen, D.-A. Trieu, C.-T. Le, V.-H. Le and N.-L. Phan, Frequency shift induced by multielectron polarization in high-order harmonic generation from polar molecules, Phys. Rev. A 111 (2025) 053101.
- [46] P. M. Kraus, D. Baykusheva and H. J. Wörner, *Two-pulse field-free orientation reveals anisotropy of molecular shape resonance*, Phys. Rev. Lett. **113** (2014) 023001.
- [47] D. T.-T. Nguyen, D. T.-D. Nguyen, D.-A. Trieu and N.-L. Phan, Effects of laser's carrier-envelope phase on electrostatic-field-induced frequency shift of high-order harmonic generation, HCMUE Journal of Science 21 (2024) 2148.
- [48] M. Abu-samha and L. B. Madsen, Single-active-electron potentials for molecules in intense laser fields, Phys. Rev. A 81 (2010) 033416.
- [49] S.-F. Zhao, C. Jin, A.-T. Le, T. F. Jiang and C. D. Lin, Determination of structure parameters in strong-field tunneling ionization theory of molecules, Phys. Rev. A 81 (2010) 033423.
- [50] V.-H. Hoang, S.-F. Zhao, V.-H. Le and A.-T. Le, *Influence of permanent dipole and dynamic core-electron polarization on tunneling ionization of polar molecules*, Phys. Rev. A **95** (2017) 023407.

[51] N.-L. Phan, K.-N. H. Nguyen, C.-T. Le, D. Vu, K. Tran and V.-H. Le, General characterization of partially oriented polar molecules by the time-frequency profile of high-order harmonic generation, Phys. Rev. A 102 (2020) 063104.